Acta Pharmaceutica Sinica B 2022;12(4):2120–2126

Chinese Pharmaceutical Association
Institute of Materia Medica, Chinese Academy of Medical Sciences

Acta Pharmaceutica Sinica B

www.elsevier.com/locate/apsb
www.sciencedirect.com

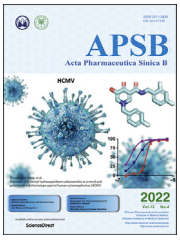

SHORT COMMUNICATION

Unraveling the drug distribution in brain enabled by MALDI MS imaging with laser-assisted chemical transfer

Shuai Guo, Kening Li, Yanwen Chen, Bin Li*

State Key Laboratory of Natural Medicines and School of Traditional Chinese Pharmacy, China Pharmaceutical University, Nanjing 210009, China

Received 22 August 2021; received in revised form 24 October 2021; accepted 3 November 2021

KEY WORDS

Pharmaceutical analysis;
Laser-assisted chemical transfer;
Mass spectrometry imaging;
Drug distribution;
Brain penetration

Abstract Accurate localization of central nervous system (CNS) drug distribution in the brain is quite challenging to matrix-assisted laser desorption/ionization (MALDI) mass spectrometry imaging (MSI), owing to the ionization competition/suppression of highly abundant endogenous biomolecules and MALDI matrix. Herein, we developed a highly efficient sample preparation technique, laser-assisted chemical transfer (LACT), to enhance the detection sensitivity of CNS drugs in brain tissues. A focused diode laser source transilluminated the tissue slide coated with α-cyano-4-hydroxycinnamic acid, an optimal matrix to highly absorb the laser radiation at 405 nm, and a very thin-layer chemical film mainly containing drug molecule was transferred to the acceptor glass slide. Subsequently, MALDI MSI was performed on the chemical film without additional sample treatment. One major advantage of LACT is to minimize ionization competition/suppression from the tissue itself by removing abundant endogenous lipid and protein components. The superior performance of LACT led to the successful visualization of regional distribution patterns of 16 CNS drugs in the mouse brain. Furthermore, the dynamic spatial changes of risperidone and its metabolite were visualized over a 24-h period. Also, the brain-to-plasma (B/P) ratio could be obtained according to MALDI MSI results, providing an alternative means to assess brain penetration in drug discovery.

*Corresponding author. Tel./fax: +86 25 83271382.
E-mail address: binli@cpu.edu.cn (Bin Li).

Peer review under responsibility of Chinese Pharmaceutical Association and Institute of Materia Medica, Chinese Academy of Medical Sciences

https://doi.org/10.1016/j.apsb.2021.11.007

1. Introduction

The total cost of drug development has more than doubled in the past decade with a high failure rate[1]. Particularly, brain drug development has proven to be very difficult, for example, the failure rate of Alzheimer's disease (AD) drug development was near 99.6%, which may hit investor confidence in innovation[2]. For central nervous system (CNS) drug discovery, one of the fundamental principles is to cross the blood–brain barrier (BBB) and distribute at the target-site at sufficient concentration to execute its pharmacological effect[3]. Several approaches have been developed for mapping brain regional distribution of small molecule drugs and assessing their brain penetration in CNS drug discovery[4]. However, accurately mapping the spatial distribution of a drug or drug candidate in the brain is not always easy, maybe even worse for micro or trace amounts of drug metabolites. Liquid/gas chromatography–mass spectrometry (LC/GC−MS) and ligand binding assay (*e.g.*, ELISA) are often used for quantitative analysis of target molecules in the biological sample[5], whereas the tissue homogenization is required resulting in the loss of spatial resolution. Whole-body autoradiography (WBA), positron emission tomography (PET), and fluorescence imaging offer the ability to visualize the tissue-specific distribution of drugs[6,7]. However, these molecular imaging techniques rely on radiolabeled tracer or report probe, which is unable to distinguish parent drug from its metabolites because only the labeled compounds can be detected[7]. Furthermore, the risk of label loss may occur in the metabolic process. Therefore, continuous development of imaging methods for precisely visualizing the distribution of small molecule drugs and their metabolites in brain tissues is critical to the research and development of CNS drugs, and non-CNS therapies, where brain penetration can cause unexpected CNS-mediated side effects[4].

Mass spectrometry imaging (MSI) appears to be a promising label-free imaging technique for interrogating the spatiotemporal distribution of endogenous compounds in various samples[8,9]. The most frequently used MSI modality is matrix-assisted laser desorption/ionization (MALDI), which has been employed to map the tissue-specific distribution of small metabolites, lipids, peptides, and proteins[10−12]. Currently, one of the most attractive applications of MALDI MSI is the visualization of tissue distribution of drug or drug candidates and their potential metabolites, providing essential spatial information for optimizing drug ADME properties[13]. However, unlike LC/GC−MS, the traditional sample purification, concentration, and chromatographic separation are not available for MSI, *in situ* detection of small molecule drugs in tissue is greatly limited by ionization competition/suppression of highly abundant endogenous biomolecules and MALDI matrix[14]. Furthermore, the amount of drug in a laser spot (∼100 μm) on a 12 μm thick tissue is significantly low (∼1 pg/spot)[15]. If the drug delivery were limited by BBB or nonspecifically and specifically bound with protein/lipid in tissue, the situation would be worse. This may be that the spatial distribution information of drug metabolite is often missed in the MSI of the parent drug.

To overcome these limitations, various strategies have been proposed for MALDI MSI of drugs to improve detection sensitivity and specificity. Discovery of novel organic matrices with high desorption/ionization (DI) of the analyte, synthesis of diverse nanomaterials, and nanostructured surfaces with low background noise and high DI efficiency have been intensively employed[16,17]. Another option to minimize salts- and lipids-induced ion suppression is tissue pretreatment with a pH-controlled buffer solution or solid hydrogel prior to MALDI MSI[18−20]. On-tissue derivatization via the introduction of the ionized group on target drug is also utilized to improve detection sensitivity in MALDI MSI[21,22]. Although several MALDI MSI methods are successfully developed based on the physicochemical properties of individual drugs, the lack of universality largely hindered their broad application to the pharmaceutical industry.

It is well-known that the detection sensitivity of drug molecules could greatly increase by extracting them from complex samples to remove the ion suppression from endogenous components. However, the *in situ* extraction method for MALDI MSI is rarely reported and quite challenging. To achieve this goal, the laser-assisted chemical transfer (LACT) technique was introduced to extract the drug molecule *in situ* from the tissue without the damage of its spatial distribution. A rationally selected MALDI matrix able to absorb the laser radiation at operational wavelength was applied as the intermediate layer to drive *in situ* extraction and chemical transfer of the target drug molecules from tissue. LACT is a chemical transfer of exogenous components, enabling universal enhancement of MALDI detection sensitivity and visualization of the spatial distribution of CNS drug and its metabolite in brain tissue.

2. Results and discussion

The prototype LACT was designed inspired by laser-assisted transfer technique[23], such as infrared laser ablation sample transfer method[24] and laser-capture microdissection technology[25]. However, they are tissue transfer methods, an indiscriminate transfer, which cannot on-tissue separate target drug molecules from endogenous components. As shown in Fig. 1A and Supporting Information Fig. S1, LACT employs a focused laser to illuminate the matrix-coated tissue placed on a donor slide in a transmission mode, and a thin film was transferred to another clean acceptor slide. The transfer is forced by strongly localized heat during laser illumination, resulting in a small volume of materials to be ablated from tissue and deposited onto the acceptor slide. LACT relies on the efficient absorption of laser energy in the tissue to obtain the optimal pattern and chemical transfer. Therefore, it is crucial to utilize a compound able to absorb laser radiation at an operational wavelength to assist chemical transfer, not tissue transfer. Ideally, if a MALDI matrix served both absorbing compounds for LACT and matrix for subsequent MALDI MSI, it could simplify the whole experiment and avoid introducing the new chemicals. Moreover, in LACT, an electric field-assisted sprayer was assembled and used to homogenously deposit matrix solution. As proved in our previous work, compared with the conventional gas spray coating method, a micro-extraction could be induced by the electric field to facilitate the analyte moving from the tissue to the matrix layer[26,27]. A desirable matrix should have a low ablation threshold and high absorption coefficient, which can effectively avoid excessive thermal effects and phase changes on tissue[28]. Therefore, the mouse after dosing of venlafaxine was sacrificed and the brain section was sprayed with five often used matrices including DHAP, THAP, DAN, DHB, and CHCA to screen the suitable matrix for LACT. A diode laser source operated at the wavelength of 405 nm was assembled on the LACT device. The solid-state absorption spectra of five candidate matrices were acquired in the range of 350−600 nm. Among them, CHCA exhibits the highest absorption at 405 nm (Fig. 1B). As expected, the lowest energy threshold for chemical transfer was 4 mW when CHCA was applied (Fig. 1C). Although tissue sections coated with the

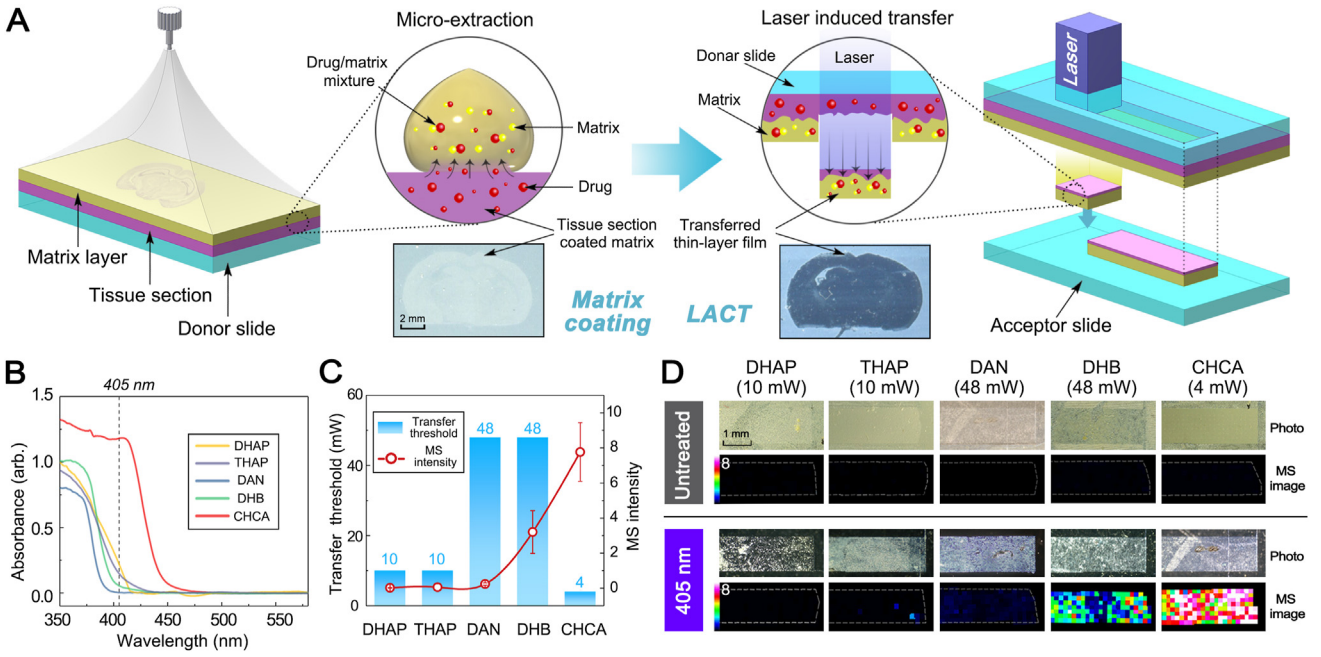

Figure 1 Working principle of LACT and optimization of absorbing matrix compound for LACT and MALDI MSI. (A) Workflow for matrix deposition, laser illumination (405 nm), and chemical transfer. (B) Solid-state UV absorption spectra of different MALDI matrices coated on brain tissues. (C) The influence of transfer threshold energy on the signal intensities of venlafaxine. The transfer threshold energy was defined as the minimum real-time power of the laser (mW) necessary to achieve chemical transfer. Error bars indicate the standard deviations of 100 mass spectra acquired from ion images. (D) Comparison of MALDI MSI results of venlafaxine measured in dosed mouse brain before and after LACT treatment using different matrices. DHAP, 2,6-dihydroxyacetophenone; THAP, 2,4,6-trihydroxy-acetophenone; DAN, 1,5-diaminonapthalene; DHB, 2,5-dihydroxybenzoic acid; CHCA, α-cyano-4-hydroxycinnamic acid.

other four matrices could be transferred using a 405 nm laser (Fig. 1D), the venlafaxine could be detected with the highest sensitivity by using CHCA-LACT (Fig. 1C and D). Herein, the optimal matching between CHCA and 405 nm laser resulted in the requirement of minimum transfer energy and greatly minimized the risk of laser-induced thermal damage. In addition, the signal intensity of venlafaxine is inversely proportional to the thickness of the transferred film (Supporting Information Fig. S2). The thinnest film (~1 μm) could be achieved using 4 mW laser radiation with the highest signal intensity of venlafaxine (Fig. S2A). Increasing laser radiation above 16 mW, the signal intensity of venlafaxine largely decreases, and the spatial distribution pattern is hardly resolved. Additionally, to remove doubt regarding the analyte delocalization possibly caused by LACT, mouse brain dosed with a fluorescent dye was firstly imaged with fluorescence microscopy, and LACT treatment was subsequently performed for MALDI MSI at 200 μm raster step size to visualize the spatial distribution of fluorescein (*m/z* 333.11). As shown in Supporting Information Fig. S3A, the spatial distribution pattern of fluorescent dye obtained by using two techniques was consistent with each other, indicating that no significant compound delocalization occurred during the LACT process. Subsequently, the raster step size of 50 μm was applied to evaluate the possible compound delocalization. The fine distribution pattern of fluorescein was resolved, which was in a blood vessel with a diameter of ~50 μm, consistent with the fluorescence image (Fig. S3A). Furthermore, brain tissues from animals dosed with imipramine were subjected to LACT for MALDI MSI of its distribution in the cerebellum (Fig. S3B). Compared to the H&E-stained image, the ion image of imipramine acquired at 50 μm step size by MALDI MSI could resolve the stripe interval between cerebellar folium (~100 μm) and the morphology of the granular layer and white matter. Additionally, a comparison of ion images of selected lipids obtained at 200 μm step size was performed on brain tissues treated with and without LACT, respectively. As shown in Fig. S3C, similar spatial distribution patterns of two selected lipids were obtained. Therefore, LACT could well preserve the spatial distribution of compound and could not cause the significant delocalization of the analytes. It can reflect the intrinsic and real distribution of molecules in tissue.

To further explore the underlying reason for the enhancement of the signal intensity of the drug by using CHCA-LACT, the potential discrimination effect in tissue transfer was investigated. LC–MS/MS analysis was performed on untreated and LACT treated tissue sections of the venlafaxine-dosed mouse brain, respectively, showing that approximately 21% of venlafaxine was extracted from the tissue and transferred to chemical film (Supporting Information Fig. S4). Moreover, the amounts of total lipids and proteins in the chemical film were determined by using sulfo-phospho-vanillin (SPV) and bicinchoninic acid (BCA) assays, respectively. As shown in Supporting Information Figs. S5 and S6, significant decreases in total lipids (64%, $P < 0.001$) and total proteins (97%, $P < 0.001$) were observed after LACT treatment. Several studies have proved that lipids and proteins could cause severe ion suppression of small molecules[29,30]. Therefore, LACT could achieve an *in situ* extraction and strips out matrix-analyte cocrystals from the tissue to separate endogenous and exogenous components. The enhancement of detection sensitivity provided by LACT was mainly attributed to the purification of the matrix-tissue layer by discarding the tissue proteins

and lipids. Consequently, ionization competition and suppression from the tissue itself was greatly minimized, which was beneficial for the detection of exogenous compounds.

Moreover, the mixture solution of CNS drug and CHCA was homogenously spray-coated on the bare ITO slide and brain tissue to evaluate tissue extinction coefficient (TEC), which is used to account for ion suppression effects that occurred in MALDI MSI[14]. TEC is calculated by comparing the mean signal intensity of a standard obtained from the tissue and bare ITO slide. The strong signal intensity of venlafaxine was obtained from bare ITO slide and chemical film, however, the venlafaxine signal was markedly suppressed by untreated brain tissue (Fig. 2A). Similar results were observed for other 15 test CNS drugs (Supporting Information Fig. S7). As shown in Fig. 2B, the average TEC value for untreated tissues of 16 CNS drugs was 0.045, similar to previous reports[14,31]. However, the average TEC value for chemical films of 16 CNS drugs was 0.76, having a ~17-fold increase. TEC results suggested that the ion suppression is mainly derived from the tissue itself, and CHCA-LACT can provide a universal enhancement effect for selected CNS drugs.

Finally, the performance of the CHCA-LACT was evaluated for its sensitivity and linearity. As shown in Fig. 2C and Supporting Information Fig. S8, >1300-fold decrease in the limit of detection (LOD) of 16 CNS drugs was observed in the chemical films as compared to the untreated tissue. Therefore, the CHCA-LACT technique can significantly improve the MALDI MS detection sensitivity of various CNS drugs due to the global minimization of ionization competition/suppression effect from abundant components in tissue. To evaluate the linearity of the method, serial dilutions of venlafaxine and lamotrigine were manually spotted on the cortex of the blank brain tissue section, respectively, and LACT was subsequently performed. The calibration curve was generated for venlafaxine and lamotrigine by plotting average signal intensities of mass spectra in a defined region of interest (ROI) as a function of the concentration of standards spotted on the brain tissue section (Supporting Information Fig. S9). The MALDI MSI results exhibited ideal linearity ($R = 0.9953$ for venlafaxine and $R = 0.9925$ for lamotrigine) within the 100-fold concentration range.

The utility of CHCA-LACT was comprehensively demonstrated by MALDI MSI of 16 CNS drugs (including 6 antipsychotic drugs, 2 anesthetic drugs, 3 antidepressant drugs, 1 antiepileptic drug, 3 anti-Alzheimer drugs, and 1 antihypertensive drug) in brain tissues from mice receiving a single dose. Meanwhile, a comparison of CHCA-LACT with the other three methods (MALDI with CHCA, MALDI with DHB, and blank control) was performed to show the advantage of CHCA-LACT in the high detection sensitivity (Fig. 3). The blank tissue treated by CHCA-LACT was used to eliminate false positive. *In situ* tandem MS/MS was performed on dosed tissues treated by CHCA-LACT to validate the identity of the drug (Supporting Information Fig. S10 and Table S2). Undoubtedly, most CNS drugs were not detectable by conventional CHCA and DHB matrices, and no interference peak was observed in blank tissue. However, with the aid of CHCA-LACT, the brain regional distributions of 16 CNS drugs were successfully revealed in the horizontal sections of the mouse brains after i.p. dosing, showing the similarity and difference in spatial distribution. Relatively high levels of drugs were detected in the cerebral cortex followed by the hippocampus, thalamus, and striatum, generally in agreement with previous studies[20,32]. Distinct distribution patterns were visualized for specific drugs. For example, quite low levels of venlafaxine, fluoxetine, and lamotrigine were observed in the cerebellum as compared with the cortex and the rest of the brain regions, which were confirmed by previous HPLC and autoradiographic methods[33–35]. These results indicate that the

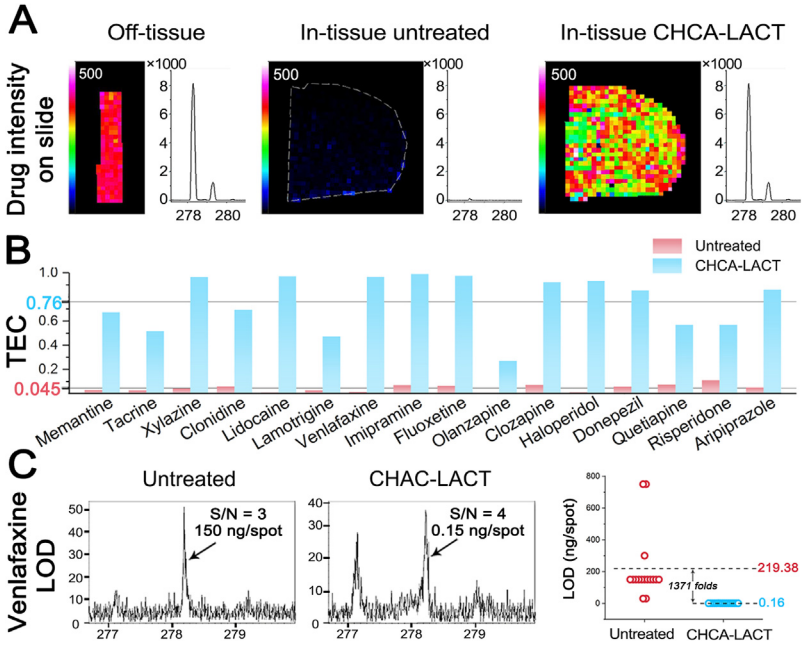

Figure 2 Evaluation of tissue extinction coefficient (TEC) and limit of detection (LOD) of CHCA-LACT technique. (A) Ion images and representative MALDI mass spectra of venlafaxine acquired from bare ITO glass slide, untreated tissue, and chemical film. (B) Histogram of calculated TEC values for each CNS drug in untreated and CHCA-LACT treated brain tissue sections. (C) Representative MALDI mass spectra of venlafaxine at LOD level and LODs of 16 CNS drugs obtained from untreated and CHCA-LACT treated tissue sections.

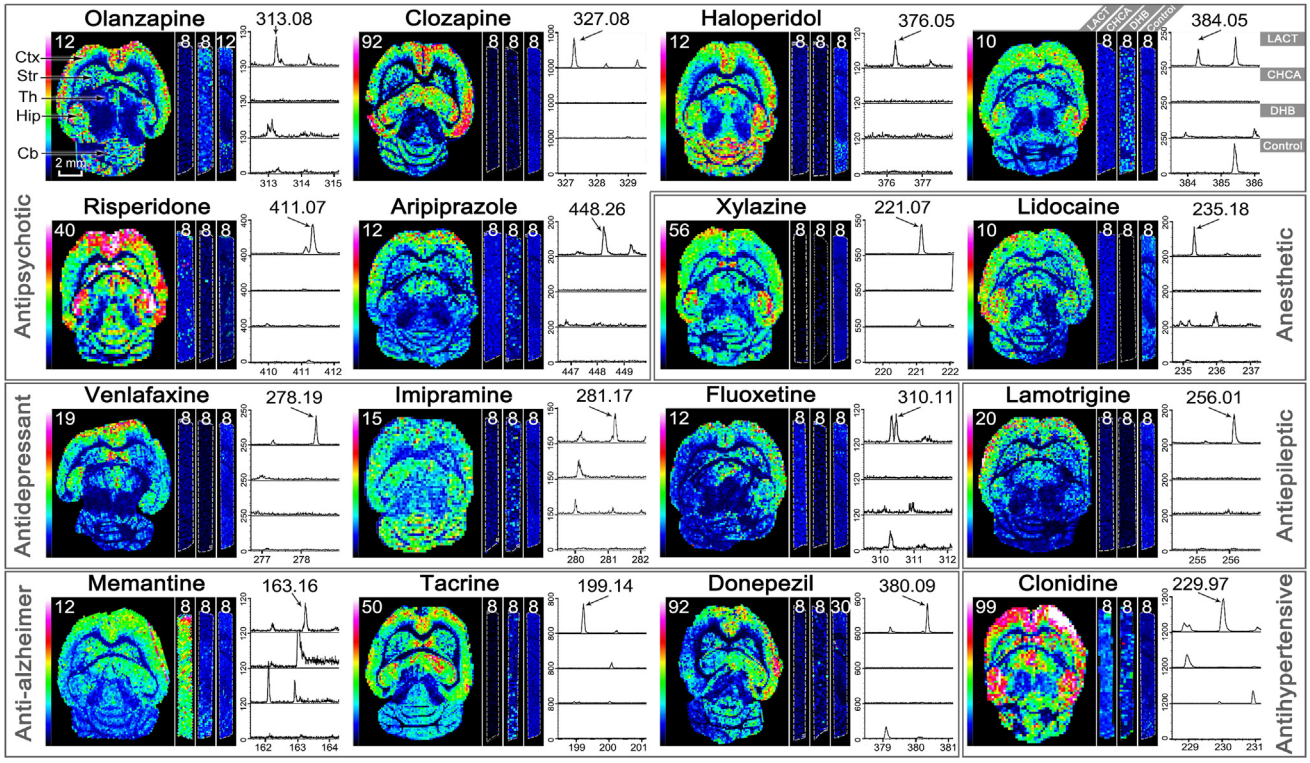

Figure 3 Comparison of the performance of three MALDI MSI methods from left to right for each CNS drug, including MALDI with CHCA-LACT (whole horizontal section), MALDI with CHCA (vertical stripe), and MALDI with DHB (vertical stripe). The blank tissue treated by CHCA-LACT was used as negative control (vertical stripe). Representative mass spectra corresponding to each imaging experiment were shown from top to bottom: MALDI with CHCA-LACT, MALDI with CHCA, MALDI with DHB, and blank control. The value of the color scale bar represents the absolute intensity divided by 10. Ctx, cerebral cortex; Str, striatum; Th, thalamus; Hip, hippocampus; Cb, cerebellum.

CHCA-LACT technique provides a universal enhancement of signal intensities of CNS drugs enable to achieve the accurate tissue-specific distributions of drugs in brain tissue. It is a very useful alternative means when the traditional MALDI MSI does not work.

The superior performance of CHCA-LACT was further demonstrated by interrogation of spatiotemporal changes of antipsychotic drug risperidone (RISP) and its metabolite in 24 h after single dosing. RISP and its one major pharmacologically active metabolite 9-hydroxy-risperidone (9-OH RISP) were readily detected by using MALDI MS with CHCA-LACT, and their spatiotemporal changes were unraveled for the first time (Fig. 4). After i.p. administration, the drug rapidly penetrated through the BBB into the brain, reaching maximum concentration (T_{max}) in ~15 min, and it was mainly observed in the frontal cortex, striatum, and hippocampus regions colocalized with the 5-HT and dopamine receptors[36]. Subsequently, tissue concentration and distribution of RISP rapidly declined by 0.5 h from peak concentration, and a small amount of parent drug was only observed in the lateral ventricles after 2 h (Fig. 4A). However, 9-OH RISP reached T_{max} in 1 h and was spatially confined in the lateral ventricles as shown in Fig. 4B. As expected, the BBB permeability of hydroxylated metabolite is lower than its parent drug. Repeatability measurements of spatiotemporal changes of RISP and 9-OH RISP in dosed mice were conducted with three biological and technical replicates (Supporting Information Fig. S11). We further validated these results by using LC–MS/MS analysis on punched tissue homogenate (Fig. 4C and D). MALDI MS and LC–MS/MS results showed a good agreement with each other in terms of brain regional concentration−time profiles and signal intensity distributions (Fig. 4D and Supporting Information Fig. S12). This experiment illustrates that MALDI MSI with CHCA-LACT provides a powerful means to accurately address the problem of tissue distribution of the drug and its metabolites. Spatiotemporal information obtained here can improve our understanding of pharmacokinetics (PK), pharmacodynamics (PD), and potential transient toxicities of RISP and its metabolite in the brain.

The extended application was finally explored by assessment of drug brain penetration to illustrate the versatility of CHCA-LACT. Brain-to-plasma (B/P) ratio, vital data for successful CNS drug development, was applied to evaluate the extent of brain uptake of 10 known CNS drugs. Taking clozapine and tacrine for example, the ion signal of plasma heme B (m/z 616.2) was utilized to segregate ion images of drugs into the brain parenchyma region and blood vessel individually (Supporting Information Figs. S13A and B). The B/P ratio was directly calculated by comparing average MS signal intensities of drugs in the brain parenchyma region to that of brain blood vessels (Fig. S13C). To validate our results, a correlation of the B/P ratio determined by MALDI MSI with CHCA-LACT and parallel artificial membrane permeability assay (PAMPA)-BBB data from literature was performed (Fig. S13D)[37,38]. As shown in Fig. S13E, the B/P ratio obtained by MALDI MSI correlated strongly with PAMPA-BBB data, with a correlation coefficient of $R = 0.8917$ and $P = 0.0005$ for 10 CNS

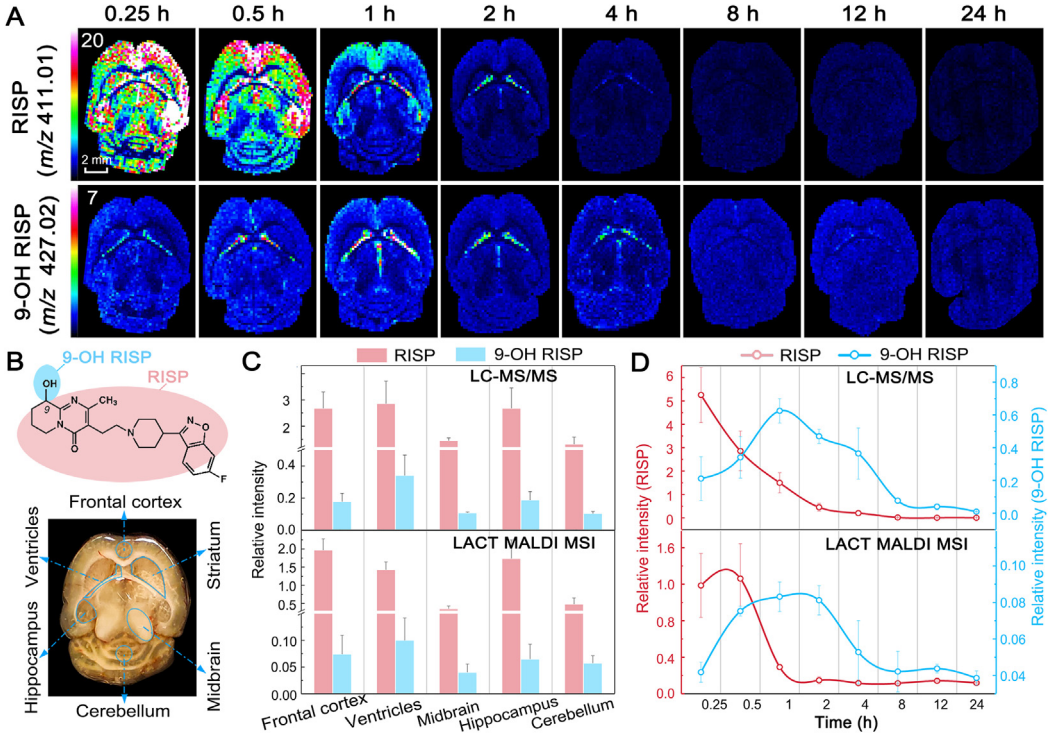

Figure 4 Visualization of spatiotemporal changes of risperidone (RISP) and its metabolite 9-hydroxy-risperidone (9-OH RISP) in brain tissues after i.p. administration using MALDI MSI with CHCA-LACT. (A) Ion images of RISP and 9-OH RISP were acquired at different time points. (B) Chemical structures of RISP and 9-OH RISP, and optical image of the horizontal section of the mouse brain. (C) Comparison of relative intensities of RISP and 9-OH RISP at different brain regions determined by LC–MS/MS and MALDI MSI with CHCA-LACT, respectively. (D) Comparison of relative intensities of RISP and 9-OH RISP in the lateral ventricles at different time points determined by LC–MS/MS and MALDI MSI with CHCA-LACT, respectively. The results were expressed as the mean ± SD from three animals.

drugs, demonstrating that MALDI MSI with CHCA-LACT could be an attractive tool for assessing brain penetration of potential CNS drug candidate.

3. Conclusions

Our work provides an efficient sample preparation technique to overcome the limitations of the current MALDI MSI. The results proved that CHCA-LACT is a powerful and universally applicable technique, which enables unraveling the spatiotemporal distribution of drugs and their metabolite in brain tissue, as well as assessing drug penetration in the brain.

Acknowledgments

This work was supported by the National Natural Science Foundation of China (Nos. 81973703 and 81803957), and the Natural Science Foundation of Jiangsu Province (No. BK20180567, China). The content is solely the responsibility of the authors and does not necessarily represent the official views of the funding agencies.

Author contributions

Shuai Guo and Bin Li: conceptualisation, investigation, methodology, validation, and writing-original draft; Kening Li and Yanwen Chen: methodology and validation; Bin Li: conceptualisation, supervision, and writing-reviewing and editing.

Conflicts of interest

The authors declare no conflict of interest.

Appendix A. Supporting information

Supporting information to this article can be found online at https://doi.org/10.1016/j.apsb.2021.11.007.

References

1. Mullard A. New drugs cost US $2.6 billion to develop. *Nat Rev Drug Discov* 2014;**13**:877.
2. Cummings JL, Morstorf T, Zhong K. Alzheimer's disease drug-development pipeline: few candidates, frequent failures. *Alzheimer's Res Ther* 2014;**6**:1–7.
3. Morgan P, Brown DG, Lennard S, Anderton MJ, Barrett JC, Eriksson U, et al. Impact of a five-dimensional framework on R&D productivity at AstraZeneca. *Nat Rev Drug Discov* 2018;**17**:167.
4. Di L, Kerns EH, Carter GT. Strategies to assess blood–brain barrier penetration. *Expet Opin Drug Discov* 2008;**3**:677–87.
5. Wong ALA, Xiang X, Ong PS, Mitchell EQY, Syn N, Wee I, et al. A review on liquid chromatography-tandem mass spectrometry methods for rapid quantification of oncology drugs. *Pharmaceutics* 2018;**10**:221.
6. McEwen A, Henson C. Quantitative whole-body autoradiography: past, present and future. *Bioanalysis* 2015;**7**:557–68.
7. James ML, Gambhir SS. A molecular imaging primer: modalities, imaging agents, and applications. *Physiol Rev* 2012;**92**:897–965.
8. Chughtai K, Heeren RM. Mass spectrometric imaging for biomedical tissue analysis. *Chem Rev* 2010;**110**:3237–77.

9. Li B, Dunham SJB, Dong Y, Yoon S, Zeng M, Sweedler JV. Analytical capabilities of mass spectrometry imaging and its potential applications in food science. *Trends Food Sci Technol* 2016;**47**:50−63.
10. Steuer AE, Poetzsch M, Kraemer T. MALDI-MS drug analysis in biological samples: opportunities and challenges. *Bioanalysis* 2016;**8**:1859−78.
11. Tang W, Gordon A, Wang F, Chen Y, Li B. Hydralazine as a versatile and universal matrix for high-molecular coverage and dual-polarity matrix-assisted laser desorption/ionization mass spectrometry imaging. *Anal Chem* 2021;**93**:9083−93.
12. Li B, Ge J, Liu W, Hu D, Li P. Unveiling spatial metabolome of *Paeonia suffruticosa* and *Paeonia lactiflora* roots using MALDI MS imaging. *New Phytol* 2021;**231**:892−902.
13. Tang W, Chen J, Zhou J, Ge J, Zhang Y, Li P, et al. Quantitative MALDI imaging of spatial distributions and dynamic changes of tetrandrine in multiple organs of rats. *Theranostics* 2019;**9**:932−44.
14. Taylor AJ, Dexter A, Bunch J. Exploring ion suppression in mass spectrometry imaging of a heterogeneous tissue. *Anal Chem* 2018;**90**:5637−45.
15. Vismeh R, Waldon DJ, Teffera Y, Zhao Z. Localization and quantification of drugs in animal tissues by use of desorption electrospray ionization mass spectrometry imaging. *Anal Chem* 2012;**84**:5439−45.
16. Wu Q, Chu JL, Rubakhin SS, Gillette MU, Sweedler JV. Dopamine-modified TiO 2 monolith-assisted LDI MS imaging for simultaneous localization of small metabolites and lipids in mouse brain tissue with enhanced detection selectivity and sensitivity. *Chem Sci* 2017;**8**:3926−38.
17. Stopka SA, Rong C, Korte AR, Yadavilli S, Nazarian J, Razunguzwa TT, et al. Molecular imaging of biological samples on nanophotonic laser desorption ionization platforms. *Angew Chem* 2016;**128**:4558−62.
18. Shariatgorji M, Kallback P, Gustavsson L, Schintu N, Svenningsson P, Goodwin RJ, et al. Controlled-pH tissue cleanup protocol for signal enhancement of small molecule drugs analyzed by MALDI-MS imaging. *Anal Chem* 2012;**84**:4603−7.
19. Song X, Luo Z, Li X, Li T, Wang Z, Sun C, et al. *In situ* hydrogel conditioning of tissue samples to enhance the drug's sensitivity in ambient mass spectrometry imaging. *Anal Chem* 2017;**89**:6318−23.
20. Chen Y, Tang W, Gordon A, Li B. Development of an integrated tissue pretreatment protocol for enhanced MALDI MS imaging of drug distribution in the brain. *J Am Soc Mass Spectrom* 2020;**31**:1066−73.
21. Shariatgorji R, Nilsson A, Fridjonsdottir E, Strittmatter N, Dannhorn A, Svenningsson P, et al. Spatial visualization of comprehensive brain neurotransmitter systems and neuroactive substances by selective *in situ* chemical derivatization mass spectrometry imaging. *Nat Protoc* 2021;**16**:3298−321.
22. Wu Q, Comi TJ, Li B, Rubakhin SS, Sweedler JV. On-tissue derivatization *via* electrospray deposition for matrix-assisted laser desorption/ionization mass spectrometry imaging of endogenous fatty acids in rat brain tissues. *Anal Chem* 2016;**88**:5988−95.
23. Serra P, Piqué A. Laser-induced forward transfer: fundamentals and applications. *Adv Mater Technol* 2019;**4**:1800099.
24. Park SG, Murray KK. Infrared laser ablation sample transfer for MALDI imaging. *Anal Chem* 2012;**84**:3240−5.
25. Espina V, Wulfkuhle JD, Calvert VS, VanMeter A, Zhou W, Coukos G, et al. Laser-capture microdissection. *Nat Protoc* 2006;**1**:586−603.
26. Guo S, Wang Y, Zhou D, Li Z. Electric field-assisted matrix coating method enhances the detection of small molecule metabolites for mass spectrometry imaging. *Anal Chem* 2015;**87**:5860−5.
27. Wang X, Han J, Yang J, Pan J, Borchers CH. Matrix coating assisted by an electric field (MCAEF) for enhanced tissue imaging by MALDI-MS. *Chem Sci* 2015;**6**:729−38.
28. Karnakis D, Lippert T, Ichinose N, Kawanishi S, Fukumura H. Laser induced molecular transfer using ablation of a triazeno-polymer. *Appl Surf Sci* 1998;**127**:781−6.
29. Boskamp MS, Soltwisch J. Charge distribution between different classes of glycerophospolipids in MALDI-MS imaging. *Anal Chem* 2020;**92**:5222−30.
30. Furey A, Moriarty M, Bane V, Kinsella B, Lehane M. Ion suppression; a critical review on causes, evaluation, prevention and applications. *Talanta* 2013;**115**:104−22.
31. Rzagalinski I, Kovacevic B, Hainz N, Meier C, Tschernig T, Volmer DA. Toward higher sensitivity in quantitative MALDI imaging mass spectrometry of CNS drugs using a nonpolar matrix. *Anal Chem* 2018;**90**:12592−600.
32. Vallianatou T, Shariatgorji M, Nilsson A, Fridjonsdottir E, Kallback P, Schintu N, et al. Molecular imaging identifies age-related attenuation of acetylcholine in retrosplenial cortex in response to acetylcholinesterase inhibition. *Neuropsychopharmacology* 2019;**44**:2091−8.
33. Murrell MD, Cruz DA, Javors MA, Thompson PM. Distribution of venlafaxine, *O*-desmethylvenlafaxine, and *O*-desmethylvenlafaxine to venlafaxine ratio in postmortem human brain tissue. *J Forensic Sci* 2014;**59**:683−9.
34. Mukherjee J, Das MK, Yang ZY, Lew R. Evaluation of the binding of the radiolabeled antidepressant drug, ^{18}F-fluoxetine in the rodent brain: an *in vitro* and *in vivo* study. *Nucl Med Biol* 1998;**25**:605−10.
35. Serralheiro A, Alves G, Fortuna A, Falcão A. Direct nose-to-brain delivery of lamotrigine following intranasal administration to mice. *Int J Pharm* 2015;**490**:39−46.
36. van Beijsterveldt LE, Geerts RJ, Leysen JE, Megens AA, Van den Eynde HM, Meuldermans WE, et al. Regional brain distribution of risperidone and its active metabolite 9-hydroxy-risperidone in the rat. *Psychopharmacology (Berl)* 1994;**114**:53−62.
37. Di L, Kerns EH, Fan K, McConnell OJ, Carter GT. High throughput artificial membrane permeability assay for blood−brain barrier. *Eur J Med Chem* 2003;**38**:223−32.
38. Di L, Kerns EH, Bezar IF, Petusky SL, Huang Y. Comparison of blood−brain barrier permeability assays: *in situ* brain perfusion, MDR1-MDCKII and PAMPA-BBB. *J Pharm Sci* 2009;**98**:1980−91.